The FASEB Journal article fj.201700573R. Published online November 16, 2017.

Reduced Dnmt3a increases Gdf5 expression with suppressed satellite cell differentiation and impaired skeletal muscle regeneration

Yukino Hatazawa,[*,†,‡,1] Yusuke Ono,[§,¶,1] Yuma Hirose,[†] Sayaka Kanai,[*] Nobuharu L. Fujii,[‖] Shuichi Machida,[#] Ichizo Nishino,[**] Takahiko Shimizu,[††] Masaki Okano,[‡‡] Yasutomi Kamei,[*,†,2] and Yoshihiro Ogawa[*,§§,¶¶,3]

[*]Department of Molecular Endocrinology and Metabolism, Graduate School of Medical and Dental Sciences, Tokyo Medical and Dental University (TMDU), Tokyo, Japan; [†]Laboratory of Molecular Nutrition, Graduate School of Environmental and Life Science, Kyoto Prefectural University, Kyoto, Japan; [‡]Japan Society for the Promotion of Science, Tokyo, Japan; [§]Musculoskeletal Molecular Biology Research Group, Nagasaki University Graduate School of Biomedical Sciences, Nagasaki, Japan; [¶]Division of Regenerative Medicine Research, Japan Agency for Medical Research and Development (AMED), Tokyo, Japan; [‖]Department of Health Promotion Sciences, Graduate School of Human Health Sciences, Tokyo Metropolitan University, Hachioji, Japan; [#]Graduate School of Health and Sports Science, Juntendo University, Chiba, Japan; [**]National Institute of Neuroscience, National Center of Neurology and Psychiatry, Tokyo, Japan; [††]Department of Advanced Aging Medicine, Chiba University Graduate School of Medicine, Chiba, Japan; [‡‡]Institute of Molecular Embryology and Genetics, Kumamoto University, Kumamoto, Japan; [§§]Department of Medicine and Bioregulatory Science, Graduate School of Medical Sciences, Kyushu University, Fukuoka, Japan; and [¶¶]Japan Agency for Medical Research and Development (AMED), Core Research for Evolutional Science and Technology (CREST), Tokyo, Japan

ABSTRACT: DNA methylation is an epigenetic mechanism regulating gene expression. In this study, we observed that DNA methyltransferase 3a (Dnmt3a) expression is decreased after muscle atrophy. We made skeletal muscle–specific Dnmt3a knockout mice (Dnmt3a-KO mice). The regeneration capacity after muscle injury was markedly decreased in Dnmt3a-KO mice. Diminished mRNA and protein expression of Dnmt3a were observed in skeletal muscles as well as in satellite cells, which are important for muscle regeneration, in Dnmt3a-KO mice. Dnmt3a-KO satellite cell showed smaller in size (length/area), suggesting suppressed myotube differentiation. Microarray analysis of satellite cells showed that expression of growth differentiation factor 5 (Gdf5) mRNA was markedly increased in Dnmt3a-KO mice. The DNA methylation level of the *Gdf5* promoter was markedly decreased in Dnmt3a-KO satellite cells. In addition, DNA methylation inhibitor azacytidine treatment increased Gdf5 expression in wild-type satellite cells, suggesting *Gdf5* expression is regulated by DNA methylation. Also, we observed increased inhibitor of differentiation (a target of Gdf5) mRNA expression in Dnmt3a-KO satellite cells. Thus, Dnmt3a appears to regulate satellite cell differentiation *via* DNA methylation. This mechanism may play a role in the decreased regeneration capacity during atrophy such as in aged sarcopenia.—Hatazawa, Y., Ono, Y., Hirose, Y., Kanai, S., Fujii, N. L., Machida, S., Nishino, I., Shimizu, T., Okano, M., Kamei, Y., Ogawa, Y. Reduced Dnmt3a increases Gdf5 expression with suppressed satellite cell differentiation and impaired skeletal muscle regeneration. FASEB J. 32, 000–000 (2018). www.fasebj.org

KEY WORDS: DNA methylation · epigenetics · atrophy · knockout mouse

Epigenetic events contribute to skeletal muscle remodeling in a variety of physiologic and pathophysiologic conditions (1). DNA methylation occurs as 5-methylcytosines mainly at cytosine–guanine dinucleotides, so-called CpG sites, and such methylation is a well-studied epigenetic mechanism for transcriptional regulation (2, 3). Generally DNA methylation of the gene promoter is correlated with transcriptional repression (2, 3). Genomic DNA methylation patterns are established by the actions of the *de novo* methyltransferases DNA methyltransferase 3a (Dnmt3a) and Dnmt3b, and are maintained by the methyltransferase Dnmt1 (4). DNA methylation has long been known to be involved in muscle formation. Treatment of fibroblasts with the DNA methylation inhibitor 5-azacytidine caused

ABBREVIATIONS: Bmp, bone morphogenic protein; CTX, cardiotoxin; Dnmt3a, DNA methyltransferase 3a; Dnmt3a-KO mice, skeletal muscle–specific Dnmt3a knockout mice; EDL, extensor digitorum longus; EdU, 5-ethynyl-2′-deoxyuridine; FGFR4, fibroblast growth factor receptor 4; Gdf, growth differentiation factor; HE, hematoxylin and eosin; IAP, intracisternal A particle; KEGG, Kyoto Encyclopedia of Genes and Genomes; KO, knockout; MyHC, myosin heavy chain; qPCR, quantitative PCR; WT, wild type; YFP, yellow fluorescent protein

[1] These authors contributed equally to this work.

[2] Correspondence: Kyoto Prefectural University, 1-5 Hangi-cho, Shimogamo, Sakyo-ku, Kyoto, 606-8522 Japan. E-mail: kamei@kpu.ac.jp

[3] Correspondence: 3-1-1 Maidashi, Higashi-ku, Fukuoka 812-8582, Japan. E-mail: yogawa@intmed3.med.kyushu-u.ac.jp

doi: 10.1096/fj.201700573R

This article includes supplemental data. Please visit *http://www.fasebj.org* to obtain this information.

muscle differentiation (5). On the other hand, deletion of *Dnmt1* in skeletal muscles is reported to reduce the differentiation capacity of myogenic cells (6). Expression of Dnmt3a mRNA is relatively high in skeletal muscles (7). Also, denervation in skeletal muscles decreased expression of Dnmt3a (8), suggesting that Dnmt3a plays a role in skeletal muscle physiology/pathophysiology, such as atrophy.

Muscle atrophy is associated with aging (sarcopenia) and chronic unloading (such as immobilization with casts), as well as nerve injury (denervation). During atrophy, the muscle regeneration capacity after injury (*e.g.*, falling, trauma, or extreme exercise) is known to be decreased (9–11). However, the mechanism involved is largely unknown. Satellite cells, the resident stem cells of adult skeletal muscles, are critical for regeneration (9), supplying myonuclei for homeostasis, hypertrophy, and replication (12). Satellite cell growth and differentiation are controlled by numerous secreted proteins, such as bone morphogenic protein (Bmp) and growth differentiation factor (Gdf), which form a family of proteins that share the characteristic features of the TGF-β family (13). Bmp/Gdf is known to activate gene expression of *Id* (inhibitor of differentiation or DNA binding) and suppress muscle differentiation (12). Previously, we examined the role of Bmp signaling in regulating satellite cell function. Blockade of Bmp signaling promoted and Bmp4 inhibited myogenic differentiation of satellite cells. Collectively, these findings suggest that Bmp signaling suppresses satellite cell differentiation (12).

Expression of *Gdf5/Bmp14* was shown to be regulated by DNA methylation at the promoter (14). Increased growth differentiation factor 5 (Gdf5) may suppress satellite cell differentiation and reduce muscle regeneration. In this study, we used mice with ablation of Dnmt3a in skeletal muscles and satellite cells, and attempted to clarify the role of DNA methylation in muscle function.

MATERIALS AND METHODS

Denervation of skeletal muscle

For the denervation model, a 4- to 5-mm section of sciatic nerve in the hind limb of wild-type (WT) mice was removed. After 14 d, skeletal muscle was collected.

Plaster cast

Plaster casts of mice were performed as previously described (15). The hind limb skeletal muscles of WT mice (9 wk old, male) were immobilized (unloaded) by a plaster cast. After 11 d, skeletal muscles were collected.

Real-time quantitative PCR analysis

Total RNA was prepared using TRIzol (Thermo Fisher Scientific, Waltham, MA, USA). cDNA was synthesized from 500 ng of total RNA using ReverTra Ace quantitative PCR (qPCR) RT MasterMix with gDNA Remover (Toyobo, Osaka, Japan). mRNA expression levels were measured on an ABI Prism 7000 (Thermo Fisher Scientific) system using Thunderbird SYBR qPCR Mix (Toyobo). The primers used are shown in Supplemental Table 1.

Dnmt3a-KO mice

We used a Cre-loxP recombination system to generate skeletal muscle–specific Dnmt3a knockout mice (Dnmt3a-KO). Dnmt3a-flox mice, originally generated in Massachusetts General Hospital (Boston, MA, USA), were provided by the Riken BRC through the National Bio-Resource Project of Mext, Japan. Briefly, mice in which exon 19 of Dnmt3a was flanked by loxP sites (16) were crossed with transgenic mice expressing Cre recombinase specifically in skeletal muscles using the human α-actin promoter (17). In addition to crossing mice homozygous for the Dnmt3a lox allele with Cre transgene (heterozygous) mice, mice homozygous for the Dnmt3a lox allele were crossed with mice without the Cre transgene. Genotyping of the Dnmt3a lox allele was performed as previously described (16), and the Cre transgene was detected with the following PCR primers: 5′-CGCCGCATAACCAGTGAAAC-3′ and 5′-ATGTCCAATTTACTGACCG-3′. Offspring of these crosses, $Dnmt3a^{flox/flox}$ with Cre (Dnmt3a-KO) and $Dnmt3a^{flox/flox}$ without Cre (WT), were used for experiments.

Western blot analysis

Western blot analysis was performed as previously described (15) using anti-Dnmt3a (H-295; Santa Cruz Biotechnology, Dallas, TX, USA) and anti-GAPDH (C14C10; Cell Signaling Technology, Danvers, MA, USA).

Histologic analyses

Skeletal muscles were frozen in liquid nitrogen–cooled isopentane. Transverse serial sections were prepared and stained with hematoxylin and eosin (HE), modified Gomori trichrome, or NADH stain, as previously described (18).

Glucose and insulin tolerance tests

Glucose tolerance tests and insulin tolerance tests were performed as previously described (15).

Muscle regeneration after cardiotoxin-induced muscle injury

Mice were injected with 50 or 100 μl of 10 μM cardiotoxin (CTX; C9759; Sigma-Aldrich, St. Louis, MO, USA) into the tibialis anterior or gastrocnemius muscle. Two weeks after injection, mice were humanely killed by cervical dislocation to collect muscle samples.

Immunostaining of skeletal muscles and satellite cells

Skeletal muscles were dissected and stained for collagen type I (red), laminin (red), and myosin heavy chain (MyHC; green). Nuclei were counterstained with DAPI (blue) (Southern Biotech, Birmingham, AL, USA). Immunocytochemistry of satellite cells and isolated single fibers was performed as previously described (12). Antibodies and suppliers are as follows: mouse anti-MyHC (MF20) (R&D Systems, Minneapolis, MN, USA), rat anti-laminin α2 (Alexis, San Diego, CA, USA), goat anti-collagen type I (Southern Biotech), anti-Pax7 (Santa Cruz Biotechnology), and anti-myogenin (F5D) (DSHB, Iowa City, IA, USA).

Primary satellite cell isolation and culture

Adult (8–12 wk old) male mice were humanely killed by cervical dislocation, and the extensor digitorum longus (EDL) muscles were isolated and digested in type I collagenase as previously described (19). Satellite cells were obtained from isolated myofibers by trypsinization in a 0.125% trypsin–EDTA solution for 10 min at 37°C. Satellite cells were cultured in growth medium (GlutaMax DMEM; Thermo Fisher Scientific) supplemented with 30% fetal bovine serum, 1% chicken embryo extract, 10 ng/ml basic fibroblast growth factor, and 1% penicillin–streptomycin. Myogenic differentiation was induced in differentiation medium (GlutaMax DMEM supplemented with 2% horse serum and 1% penicillin–streptomycin) (19).

Fluorescent reporter mice (Rosa-stop-YFP mice) of Cre expression

The Rosa-stop-YFP mouse is a reporter system that expresses yellow fluorescent protein (YFP) only in cells expressing Cre recombinase and their daughter cells. It was created by inserting YFP cDNA preceded by a loxP flanked "stop" sequence into the ubiquitously expressed ROSA26 locus (20). Mice with the Cre transgene driven by the α-actin promoter were crossed with fluorescent reporter mice (Rosa-stop-YFP mice). Muscle fibers were isolated as previously described (12). Satellite cells were stained with the cell marker Pax7. Mouse anti-Pax7 was used for immunostaining. Pax7-positive cells on muscle fibers from actin-Cre/Rosa-YFP floxed mice emitting a strong YFP signal were considered to be satellite cells with an active Cre system.

Analysis of cell proliferation

In experiments measuring cell proliferation, the Click-iT Plus 5-ethynyl-2′-deoxyuridine (EdU) Alexa Fluor 488 Flow Cytometry Assay Kit (Thermo Fisher Scientific) was used as per the manufacturer's instructions. EdU stock solution (10 mM) was added to the culture up to a 10 μM final concentration and subsequently cultured for an additional 6 h. Immunostained myofibers and plated myoblasts were viewed on an inverted laboratory microscope with LED Illumination Leica DM IL LED. Digital images were acquired with a Leica DFC3000 G system using Leica LAS Image Overlay 4.6 software (Leica, Wetzlar, Germany), optimized, and assembled into figures using ImageJ software (Image Processing and Analysis in Java; National Institutes of Health, Bethesda, MD, USA; *http://imagej.nih.gov/*).

cDNA microarray analysis

RNA was isolated from satellite cells from Dnmt3a-KO or WT mice. Each sample was labeled with cyanine 3-CTP using the Low Input Quick Amp Labeling Kit (Agilent Technologies, Santa Clara, CA, USA) and hybridized to the Agilent whole mouse genome (4 × 44 K) microarray. Signal detection and data analysis were performed as previously described (21).

Functional annotation analysis in genes regulated by Dnmt3a-KO

We conducted pathway analysis using the Kyoto Encyclopedia of Genes and Genomes (KEGG) database resource with Database for Annotation, Visualization and Integrated Discovery (DAVID), which is a Web application providing a comprehensive set of functional annotation tools to understand the biologic meaning of a large list of genes (21). A list of gene symbols that showed changed expression in satellite cells of Dnmt3a-KO mice was submitted, and a significant over-representation of the KEGG pathway was detected (21).

Gdf5 protein concentration analysis

Concentrations of Gdf5 in culture medium, which was precipitated with trichloroacetic acid and dissolved in water, were measured by an ELISA kit (mouse GDF-5 DuoSet; R&D Systems).

Bisulfite DNA methylation analysis

Genomic DNA was isolated by a standard procedure using proteinase K treatment. Bisulfite DNA methylation analysis was performed as previously described (22). PCR amplification of the genes of interest was performed using the following specific primers: Gdf5 forward: TTTTAGGAGGTGGAGGTGAAAATT, reverse: ACTTATATAAAACTAAAAAATTTTTCCAAAAA; intracisternal A particle (IAP) forward: TTGATAGTTGTGTTTTAAGTGGTAAATAAA, reverse: AAAACACCACAAACCAAAATCTTCTAC. QUMA (a Web-based quantification tool for methylation analysis) (*http://quma.cdb.riken.jp/*) (23) was used for bisulfite sequencing analysis of CpG methylation. Representative data of 3 independent experiments with similar results are shown in the figures.

Treatment of satellite cells by DNA methylation inhibitor 5-azacytidine

Satellite cells were isolated from the EDL of WT mice (8 wk old, male). After isolation, satellite cells were cultured for 6 d. On day 4, 5-azacytidine was treated with medium (5 μg/ml). On day 6, satellite cells were replated and cultured in differentiation medium containing 5 μg/ml 5-azacytidine for 1 d.

Gdf5 recombinant protein

Satellite cells were cultured in growth medium for 6 d, replated, and cultured in differentiation medium containing 10 or 100 ng/ml Gdf5 recombinant protein (Peprotech, Rockyhill, NJ, USA) for 2 d.

Genomewide analysis of DNA methylation

Microarray-based integrated analysis of methylation by isoschizomers analysis, a genomewide analysis of DNA methylation using a gene array and methylation-sensitive restriction enzymes, was performed as previously described (22). Briefly, genomic DNA from the two samples was digested using the methylation-sensitive *Hpa*II and methylation-insensitive *Msp*I, followed by adaptor ligation and PCR amplification. Amplified DNA from 1 sample was labeled with Cy3 and the other with Cy5; further, they were cohybridized in the gene arrays containing 41,332 probes. The difference in the *Hpa*II/*Msp*I signal was used to determine the degree of methylation (22).

Statistical analyses

Sample sizes were not based on power calculations. No animals were excluded from analyses. Statistical comparison of two groups was performed by Student's 2-tailed unpaired Student's *t*

test or a 1-way analysis of variance followed by Tukey's *post hoc* test for more groups. Data were checked for normality and equal variances between groups. A value of $P < 0.05$ was considered to be significant, and significance was indicated as $*P < 0.05$, $**P < 0.01$, and $***P < 0.001$. The number of animals in each experiment is stated in the respective figure captions. All *in vitro* experiments were replicated 2 to 4 times, and the main animal experiments were conducted twice.

RESULTS

Decreased Dnmt3a mRNA expression in multiple skeletal muscle atrophy models

Histochemical analysis (HE staining) of the atrophied skeletal muscles from different mouse models (denervation, plaster cast, and aging) demonstrated a reduction in muscle fiber size (Supplemental Fig. 1). We examined the mRNA expression levels of DNA methyltransferases (Dnmt1, Dnmt3a, and Dnmt3b), and histone methylases (Ehmt1, Ehmt2, and Ezh2) in skeletal muscles of multiple atrophy models by qPCR. Dnmt3a mRNA expression was decreased in all atrophy models (denervation, plaster cast, and aging), while expression levels of Dnmt1, Dnmt3b, and histone methylases were not significantly altered (**Fig. 1*A*–*C***). A previous study showed a decrease in Dnmt3a protein expression in muscle after denervation (8). Also, our Western blot data revealed a decrease in Dnmt3a protein expression in an aging-caused muscle atrophy (Supplemental Fig. 2). Thus, Dnmt3a may play a role in skeletal muscle biology.

Creation of mice with deletion of Dnmt3a specifically in skeletal muscles

To examine the role of Dnmt3a in skeletal muscles, we produced skeletal muscle–specific Dnmt3a knockout (Dnmt3a-KO) mice. We used a Cre-loxP recombination system of transgenic mice expressing Cre recombinase using the human *α-actin* promoter. A typical genotyping result is shown in **Fig. 2*A***. In skeletal muscles of Dnmt3a-KO mice, Dnmt3a mRNA expression was reduced to ~10% of WT levels (Fig. 2*B*). On the other hand, mRNA expression of Dnmt3a was not decreased in other tissues (Fig. 2*B*). We then confirmed decreased Dnmt3a protein expression in skeletal muscles, but not the liver (Fig. 2*C*). Expression of Dnmt1 and Dnmt3b mRNAs did not differ between WT and Dnmt3a-KO mice in skeletal muscles (Fig. 2*D*). The *α-actin* promoter driving the *Cre* transgene in our Dnmt3a-KO mice acts after birth (17). Indeed, decreased Dnmt3a mRNA expression was not observed in the whole embryo at E13.5 or in the hind limbs (containing skeletal muscles) at E18.5 of Dnmt3a-KO mice (data not shown).

Skeletal muscles of Dnmt3a-KO mice appear normal

We did not observe gross morphologic differences between Dnmt3a-KO and WT mice. Body and tissue weights (including of the gastrocnemius and quadriceps muscles, liver, and white adipose tissue) did not differ between WT and Dnmt3a-KO mice (**Fig. 3*A***), and there were no gross structural abnormalities in skeletal muscle tissue sections stained with HE (Fig. 3*B*). Similarly, additional histologic analyses using modified Gomori trichrome and NADH staining did not reveal marked differences in skeletal muscles of Dnmt3a-KO mice compared to WT mice (Fig. 3*C, D*). We also did not observe signs of muscle degeneration in Dnmt3a-KO mice. Moreover, Dnmt3a-KO mice have a similar capacity to WT mice for glucose metabolism in skeletal muscles (Fig. 3*E, F*).

Suppressed regeneration of skeletal muscles in Dnmt3a-KO mice

DNA methylation is known to be involved in muscle cell differentiation (5). Thus, we focused on a condition where the activity of muscle cell (satellite cell) differentiation is high, such as muscle regeneration. During atrophy, Dnmt3a expression is decreased and muscle regeneration is impaired (9) (Supplemental Fig. 3). We then injected CTX in skeletal muscles of Dnmt3a-KO mice to activate satellite cells. Centronuclear cells, which appear during muscle regeneration (24), were observed in muscle sections from WT mice after CTX injection (Fig. 3*G*), indicating normal regeneration. In muscle samples from Dnmt3a-KO mice, centronuclear cells were surrounded by more stromal cells (Fig. 3*G*). Collagen type I, a marker of fibrogenesis, was observed in skeletal muscles of Dnmt3a-KO mice after CTX injection (Fig. 3*H*), indicating impaired regeneration. Laminin and MyHC staining showed that muscle fiber size was smaller in Dnmt3a-KO mice than in WT mice, followed by CTX injection (Fig. 3*H*). We quantified the cross-sectional area of the muscle fibers containing centralized nuclei (a feature of nascent myofibers) using laminin/DAPI staining. Fibers with centralized nuclei were smaller in Dnmt3a-KO mice than in WT mice (Fig. 3*H*). Moreover, the decrease in muscle mass after CTX injection was larger in Dnmt3a-KO mice than in WT mice (Fig. 3*I*), also indicating suppressed regeneration in Dnmt3a-KO mice.

Deletion of Dnmt3a in satellite cells from Dnmt3a-KO mice

Next, we examined whether Dnmt3a is deleted in satellite cells. Thus, we examined the expression of Dnmt3a in satellite cells isolated from Dnmt3a-KO mice. We observed a marked decrease in Dnmt3a mRNA in Dnmt3a-KO satellite cells compared to WTs (**Fig. 4*A***), as well as reduced Dnmt3a protein expression (Fig. 4*B*), while neither Dnmt1 nor Dnmt3b mRNA levels differed significantly between genotypes (Fig. 4*A*). We also observed Cre mRNA expression in Dnmt3a-KO satellite cells (Fig. 4*A*).

To our knowledge, there are no reports that the *α-actin* promoter is active in satellite cells. We next examined

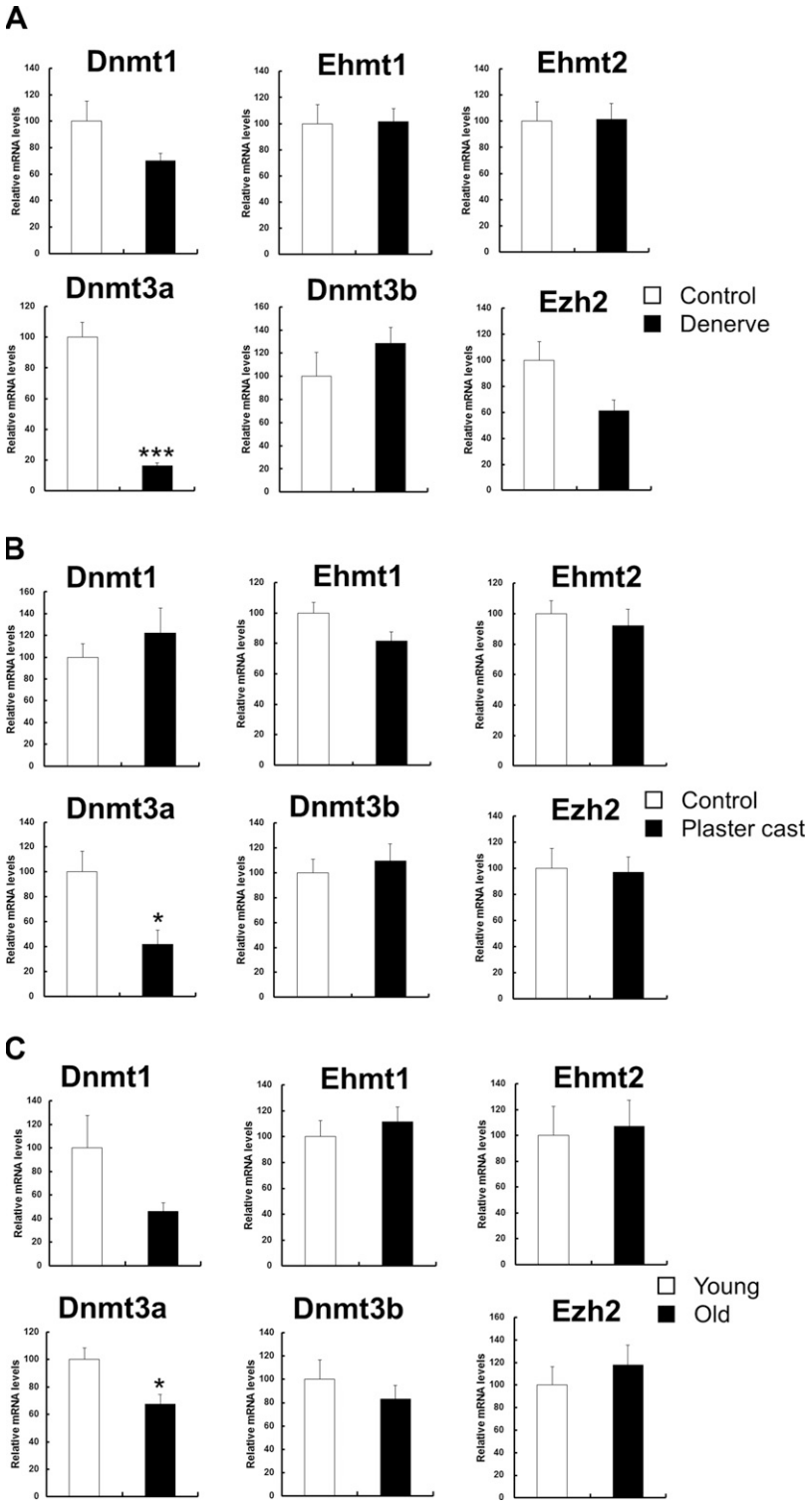

Figure 1. Decreased Dnmt3a expression in mouse skeletal muscles atrophied by denervation, plaster cast immobilization, or aging. mRNA expression in mouse skeletal muscles atrophied by denervation, $n = 6$ each group (*A*), plaster cast immobilization, $n = 6$ each group (*B*), or aging (*C*); young (13 wk old): $n = 4$, old (25 mo old); $n = 5$. Data are presented as means ± SEM. $^{*}P < 0.05$, $^{***}P < 0.001$ (unpaired, 2-tailed Student's *t* test).

whether *α-actin* promoter-driven Cre is functional in satellite cells *in vivo* using a reporter system (20). Almost all Pax7-positive satellite cells in muscle fibers from *α-actin*-Cre/Rosa-YFP floxed mice emitted strong YFP fluorescence, indicating that the *α-actin* promoter was active in satellite cells (Fig. 4*C*). This suggests that the Cre-loxP system works successfully in satellite cells derived from Dnmt3a-KO mice *in vivo*. A genomewide analysis of DNA methylation using a gene array (microarray-based integrated analysis of methylation by isoschizomers analysis) showed a reduction in the extent of DNA methylation in several gene regions in the satellite cells of Dnmt3a-KO mice (Supplemental Table 2), confirming that the Dnmt3a deletion is indeed functional. Thus, Dnmt3a-KO mice show Dnmt3a deletion in satellite cells as well as in skeletal muscles.

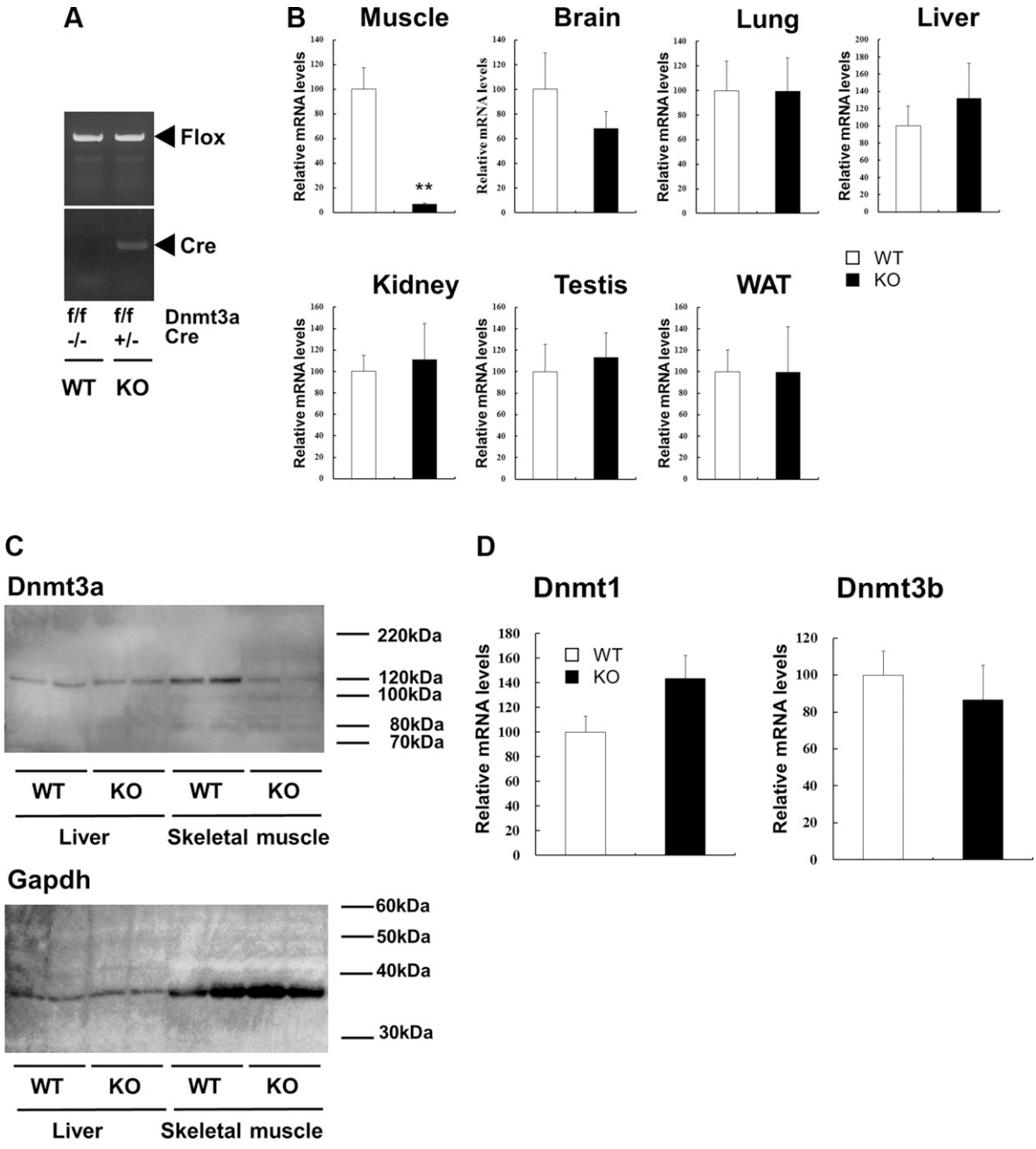

Figure 2. Expression of Dnmt3a in skeletal muscles of Dnmt3a-KO mice. *A*) Genotyping of Dnmt3a-KO mice. PCR analysis with tail genomic DNA from WT or Dnmt3a-KO. *B*) Expression of Dnmt3a mRNA in various tissues from Dnmt3a-KO mice and WT littermates by qPCR; $n = 3$ each group. *C*) Protein levels of Dnmt3a and control Gapdh in skeletal muscles and liver of Dnmt3a-KO and WT mice by Western blot analysis. Typical blots are shown; $n = 2$ each group. *D*) Expression of Dnmt1 and Dnmt3b mRNA in skeletal muscles of Dnmt3a-KO mice assessed by qPCR. Same tissue samples as in (*B*). Data are presented as means ± SEM. $^{**}P < 0.01$ (unpaired, 2-tailed Student's *t* test).

Cell morphology in satellite cells of Dnmt3a-KO mice

Because Dnmt3a is absent in satellite cells obtained from Dnmt3a-KO mice (Fig. 4*A, B*), we compared the phenotype of satellite cells isolated from Dnmt3a-KO mice with that of satellite cells isolated from WT mice. The morphology of the satellite cells obtained from Dnmt3a-KO mice appeared distinct from those of WT mice *in vitro* (**Fig. 5*A***). To determine the phenotype of the satellite cells from Dnmt3a-KO mice, we performed immunostaining of the cell-stage markers. Cell proliferation (assessed by Edu incorporation in Pax7-positive–satellite cells; Fig. 5*B*) and myogenin staining [a commitment marker of myocyte (25), Fig. 5*C*], were similar between Dnmt3a-KO and WT cells. Meanwhile, Dnmt3a-KO cells had a decreased number of nuclei in the myotubes (myonuclei) (Fig. 5*D, E*), suggesting that the fusion index is lower in Dnmt3a-KO than in WT cells. Cell length of MyHC-positive

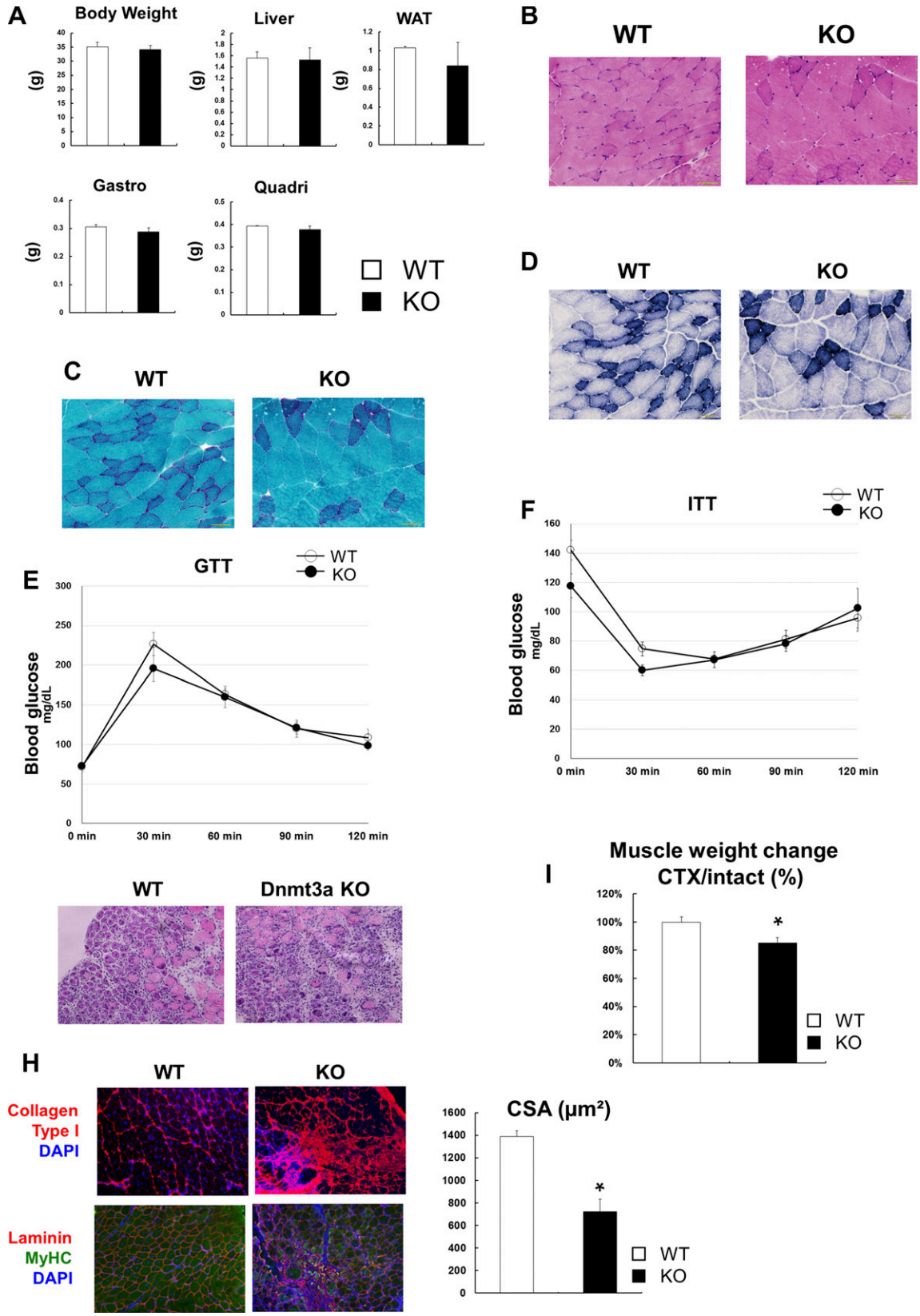

Figure 3. Skeletal muscle-related phenotype of Dnmt3a-KO mice. *A*) Dnmt3a-KO (16–18 wk old, males) and age- and sex-matched WT littermates were allowed *ad libitum* access to food. Whole body weight and weights of liver, white adipose tissue (WAT), and skeletal muscles (gastrocnemius, quadriceps) are shown; $n = 3$ each group. *B–D*) Histologic analysis of skeletal muscles of WT and Dnmt3a-KO mice. Structure of muscle cross sections was analyzed by histologic staining; HE (*B*), modified Gomori trichrome (*C*), and NADH (*D*) staining. There were no marked structural differences between Dnmt3a-KO and WT mice skeletal muscles. *E, F*) Glucose tolerance test (*E*) and insulin tolerance test (*F*) showed similar glucose metabolism between

(*continued on next page*)

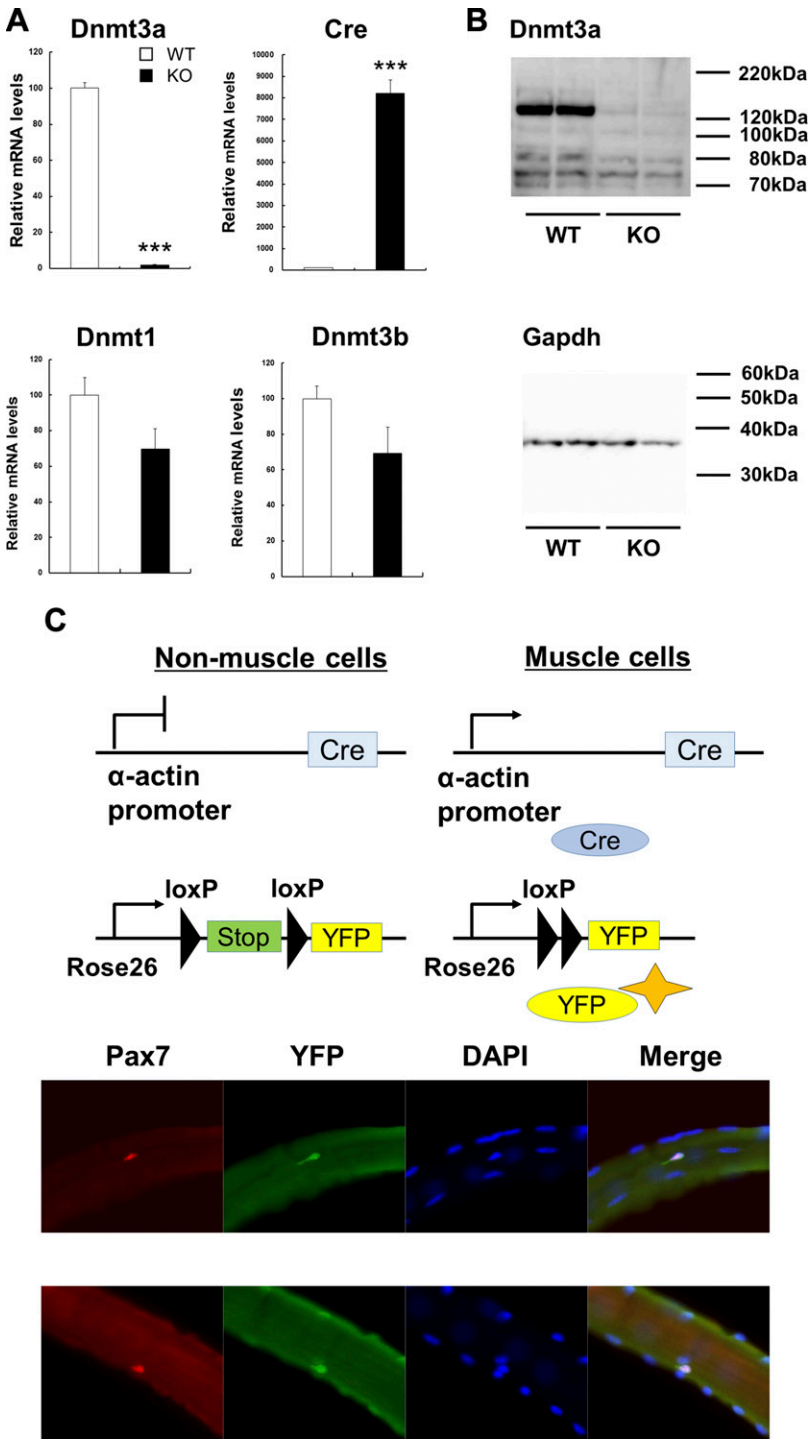

Figure 4. Decreased expression of Dnmt3a in satellite cells from Dnmt3a-KO mice. Satellite cells were isolated from EDL muscle of Dnmt3a-KO mice and WT littermates. Satellite cells were then cultured in growth medium for 6 d and differentiation medium for 2 d. *A*) mRNA expression profiles of satellite cells from Dnmt3a-KO mice by qPCR; $n = 3$–4 each group. *B*) Protein levels of Dnmt3a and control Gapdh in satellite cells derived from Dnmt3a-KO and WT mice; $n = 2$ each group. *C*) Schematic diagram of fluorescent reporter mice (Rosa26-stop-YFP) system (top). In absence of Cre expression (nonmuscle cells), YFP does not emit fluorescence signals because of stop codon in front of gene. In presence of Cre expression (muscle cells), stop codon is removed and YFP can emit fluorescence signals. Pax7-positive quiescent satellite cells in myofibers freshly isolated from EDL muscle of α-actin–Cre mice crossed with fluorescent reporter mice (Rosa26-stop-YFP mice) emitted strong YFP signals (bottom). Data represent means ± SEM. $***P < 0.001$ (unpaired, 2-tailed Student's *t* test).

myotubes was shorter in Dnmt3a-KO than WT cells (Fig. 5*D, E*). In addition, the MyHC-positive myotube area per microscopic field was smaller (Fig. 5*D, E*), suggesting myogenic differentiation was impaired or delayed in Dnmt3a-KO compared to WT cells. As myotube formation was delayed (smaller cell area) in Dnmt3a-KO cells, muscle regeneration was likely impaired.

WT and Dnmt3a-KO mice. *G*) Skeletal muscles of WT and Dnmt3a-KO mice were injured by injection of CTX. After 2 wk, skeletal muscles were stained with HE. Representative images of stained muscles cross sections are shown; $n = 6$ each group. *H*) Skeletal muscles were stained for collagen type I (red), laminin (red), and MyHC (green). Nuclei were counterstained with DAPI (blue). Separate cohort of animals ($n = 8$) from those used in *G* was used. Cross sectional area (CSA) of representative muscle fibers with centralized nuclei (a feature of nascent myofibers) from each group, obtained after laminin/DAPI staining, is shown in graph; $n = 3$. *I*) Muscle weight (2 wk after CTX injection) was measured. Same samples as used in *H*; $n = 5$ each group. Data represent means ± SEM. $*P < 0.05$ (unpaired, 2-tailed Student's *t* test).

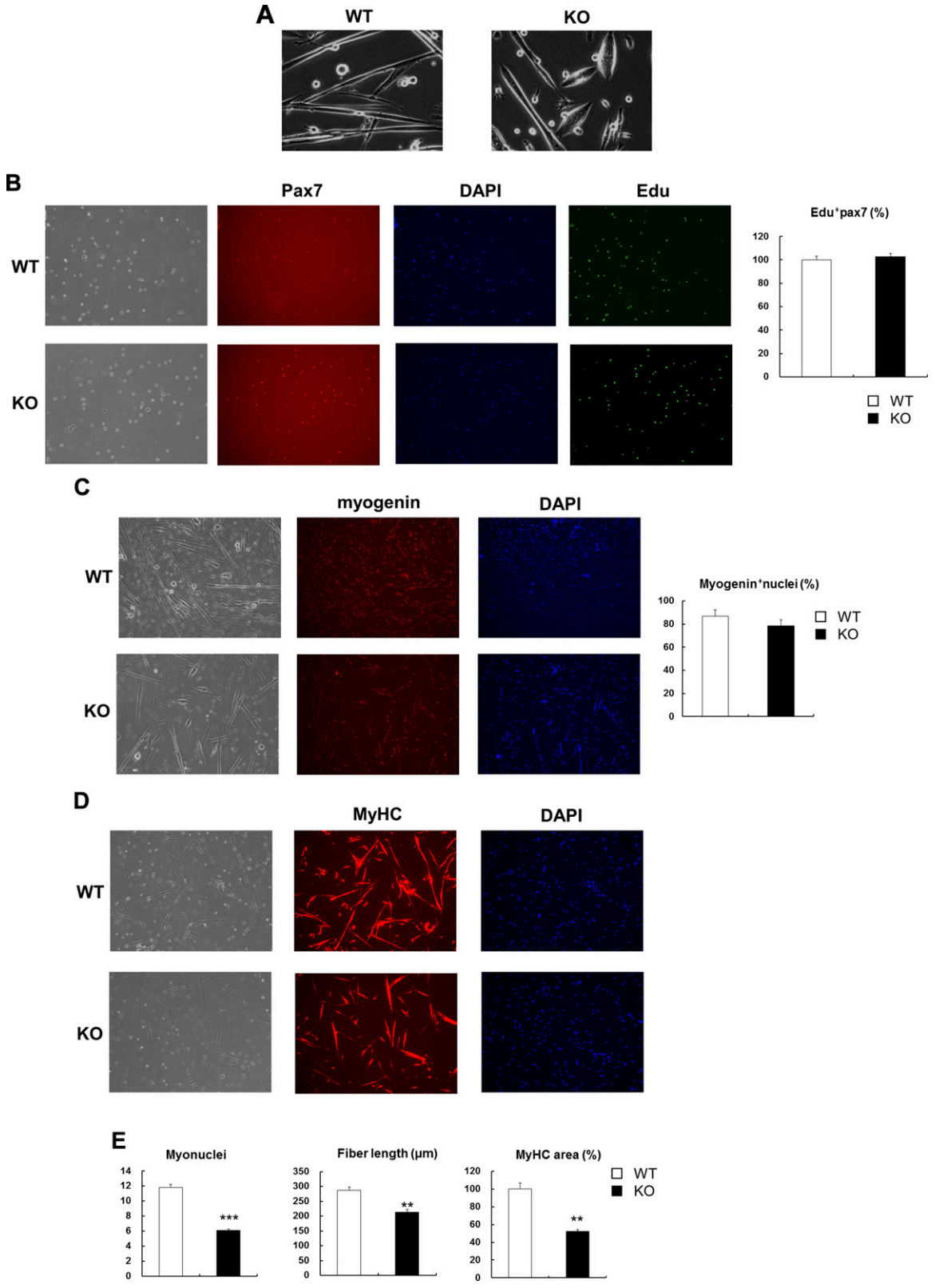

Figure 5. Morphology and immunohistochemistry in satellite cells from Dnmt3a-KO mice. *A*) Microscopic bright field view. Satellite cells isolated from EDL of Dnmt3a-KO mice and WT littermates. Cells were cultured in growth medium for 6 d and in differentiation medium for 3 d, and morphology was observed microscopically. Typical pictures are shown; $n = 3$ per group. *B*) Satellite cells were cultured in growth medium for 3 d. Immunostaining of Pax7 (red) in Dnmt3a-KO and WT satellite cells, and Edu (green) incorporation per Pax7-positive cell during cell proliferation are shown. Nuclei were stained with DAPI (blue). *C, D*) Satellite cells were cultured in growth medium for 6 d, replated with cell number matching, and in differentiation medium for 2 d. *C*) Immunostaining of myogenin (red) in myotubes from Dnmt3a-KO and WT satellite cells. Ratio of myogenin-positive cells

(*continued on next page*)

TABLE 1. *Microarray analysis of satellite cells derived from Dnmt3a-KO and WT genes showing >2-fold increase in Dnmt3a-KO compared to WT-derived satellite cells*

Gene	Description	KO/WT, d			
		2	4	5	6
Gdf5	Growth differentiation factor 5 (Gdf5)	7.1	6.9	6.1	3.9
LOC100045886	Hypothetical protein LOC100045886 (LOC100045886)	4.3	3.0	3.4	2.4
Tchh	Trichohyalin (Tchh)	4.3	3.0	2.3	2.4
Gm3866	Hypothetical protein LOC100042484 (LOC100042484)	3.1	3.8	3.7	4.0
2200002D01Rik	RIKEN cDNA 2200002D01 gene (2200002D01Rik)	2.5	2.2	4.7	2.7
Zmynd17	Zinc finger, MYND domain containing 17 (Zmynd17)	2.3	2.5	2.2	2.2
Svop	SV2 related protein (Svop)	2.2	5.5	2.7	2.4
Ctxn3	Cortexin 3 (Ctxn3)	2.0	2.0	2.2	2.1

Satellite cells were isolated from the EDL of Dnmt3a-KO mice and age- and sex-matched WT littermates. After isolation, satellite cells were cultured in growth medium for 5 d, replated with cell number matching, and cultured in differentiation medium for 2, 4, 5, and 6 d. Satellite cells were collected and global gene expression analyzed by microarray. List of up-regulated genes (more than 2-fold compared to WT mice) in all samples.

Gdf5 expression in satellite cells of Dnmt3a-KO mice

To examine gene expression changes in satellite cells derived from Dnmt3a-KO mice, we performed microarray analysis. The list of genes showing a >2-fold increase in Dnmt3a-KO compared to WT-derived satellite cells is shown in **Table 1**. Expression of growth differentiation factor 5 (Gdf5)/bone morphogenic protein 14 (Bmp14) mRNA was most markedly increased in satellite cells derived from Dnmt3a-KO mice compared to WT mice. Because Gdf5 is the most markedly up-regulated gene in satellite cells of Dnmt3a-KO mice, we focused on Gdf5. We observed increased Gdf5 mRNA expression in satellite cells of Dnmt3a-KO mice by qPCR (**Fig. 6*A***). The list of genes that were up-regulated more than 1.3-fold is shown in Supplemental Table 3. Furthermore, we performed bioinformatics analysis to understand the function of these listed genes. In the list of up-regulated genes, we detected the TGF-β signaling pathway (**Table 2**). Because Gdf5 belongs to the TGF-β superfamily, these data also support our focus on Gdf5 as an important factor for the Dnmt3a-related phenotype. In addition, we confirmed the mRNA expression of the receptors for Gdf5 in the satellite cells (Supplemental Fig. 4). Moreover, the Gdf5 protein concentration was higher in the medium of satellite cell cultures from Dnmt3a-KO mice than that of WT mice, as measured by ELISA (Fig. 6*B*), suggesting that reduced Dnmt3a expression enhances Gdf5 protein expression and secretion.

DNA methylation level of *Gdf5* gene promoter in satellite cells of Dnmt3a-KO mice

Generally DNA methylation of the gene promoter is correlated with transcriptional repression (2, 3). The human *GDF5* promoter was reported to be regulated by DNA methylation. The proximal promoter region of the *GDF5* gene (from −0.5 to 0 kb relative to the transcription start site) in particular is thought to strongly regulate gene expression (14). Supplemental Fig. 5*A* presents a schematic representation of the mouse *Gdf5* promoter with CpG positions. A homology search between the human *GDF5* and mouse *Gdf5* promoter at −0.5 kb showed high homology and included most CpG sequences (Supplemental Fig. 5B). We then compared the DNA methylation level of the *Gdf5* promoter in satellite cells derived from Dnmt3a-KO and WT mice. Interestingly, bisulfite analysis revealed much lower DNA methylation of the *Gdf5* promoter in satellite cells derived from Dnmt3a-KO mice compared to WT mice (Fig. 6*C, D*), whereas the IAP region remained methylated in satellite cells of both Dnmt3a-KO and WT mice (Fig. 6*C, E*). Deletion of Dnmt3a did not reduce DNA methylation nonspecifically in satellite cells. We then treated WT satellite cells with 5-azacytidine, a DNA methylation inhibitor (5). Treatment with 5-azacytidine increased the expression of Gdf5 mRNA but did not affect the expression of other, unrelated genes such as those of ribosomal 36B4 and muscle pyruvate kinase (Fig. 6*F*). Thus, DNA methylation appears, at least in part, to be involved in the regulation of *Gdf5* expression in satellite cells.

Gene expression in satellite cells of Dnmt3a-KO mice

The list of genes down-regulated to <0.5-fold in Dnmt3a-KO compared to WT-derived satellite cells by microarray analysis is shown in **Table 3**. The mRNA expression levels of the mature muscle marker proteins [*i.e.*, myosin heavy chain (Myh)6, Myh7 (26), and

per nucleus is shown in graph. *D*) Immunostaining of MyHC (red) in myotubes from Dnmt3a-KO and WT satellite cells. *E*) Nucleus number of myotube (myonuclei), myotube length, and ratio of MyHC-positive area per microscopic field are shown. More than 100 myotubes per well were counted in random fields; $n = 6$ (6 individual wells). Data represent means ± SEM. $^{**}P < 0.01$, $^{***}P < 0.001$ (unpaired, 2-tailed Student's t test).

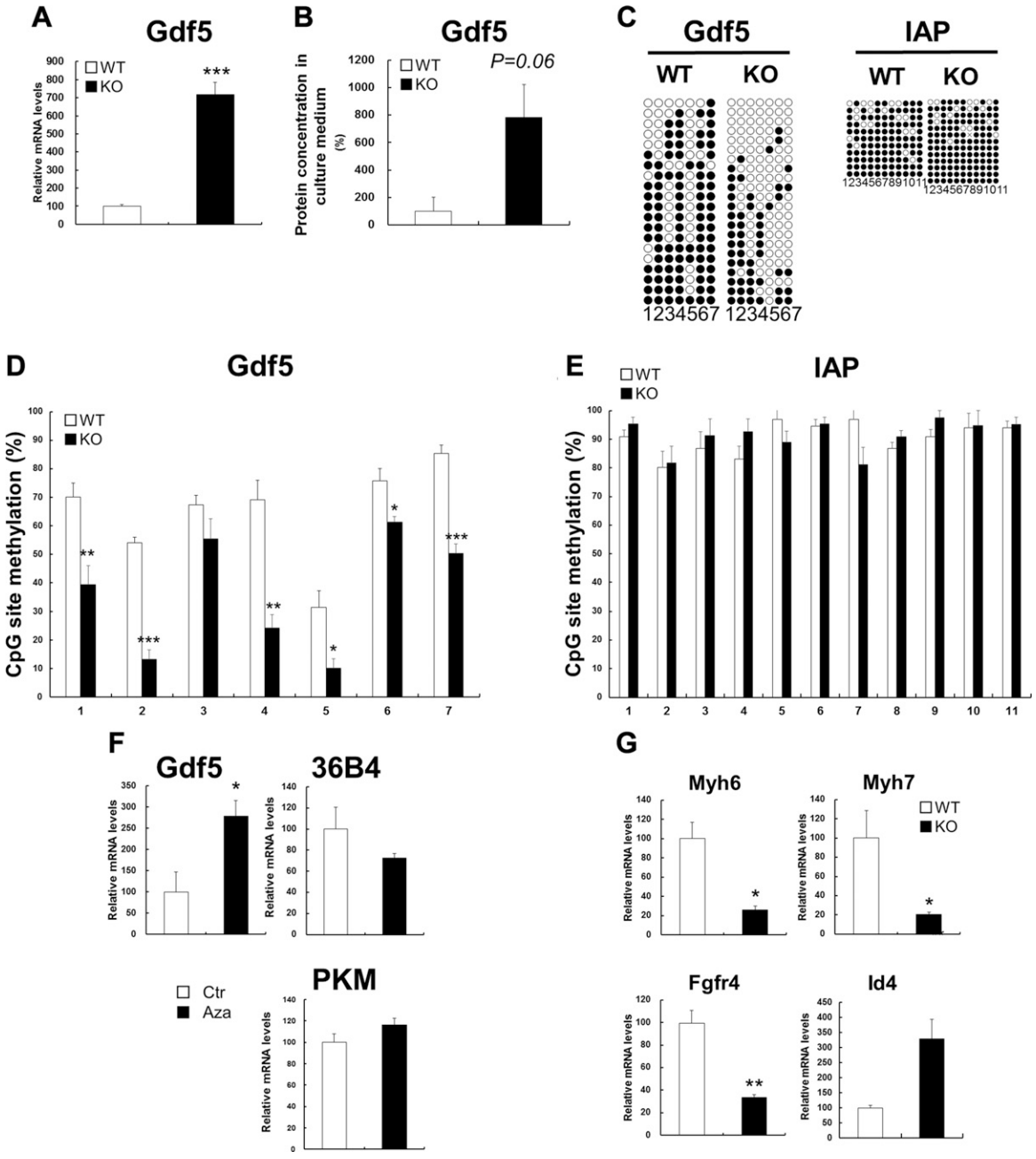

Figure 6. Increased expression of Gdf5 and decreased DNA methylation level of *Gdf5* promoter in satellite cells from Dnmt3a-KO mice. *A*) Expression of Gdf5 mRNA in satellite cells from Dnmt3a-KO mice, analyzed by qPCR; $n = 3$–4 each group. *B*) Protein level of Gdf5 in culture medium of satellite cells from Dnmt3a-KO mice, measured by ELISA; $n = 3$ each group. *C*) Bisulfite analysis of *Gdf5* promoter and IAP region in satellite cells from Dnmt3a-KO or WT mice. *D*, *E*) Quantification of bisulfite data shown in *C*. *D*) Gdf5, *E*) IAP; $n = 3$ each group. *F*) mRNA expression of Gdf5, 36B4, and pyruvate kinase muscle (PKM) in satellite cells from WT mice in presence of DNA methylation inhibitor 5-azacytidine. *G*) Differential expression of representative genes identified by microarrays was confirmed by qPCR; $n = 3$ each group. Data represent means ± SEM. $^*P < 0.05$, $^{**}P < 0.01$, $^{***}P < 0.001$ (unpaired, 2-tailed Student's t test).

fibroblast growth factor receptor 4 (FGFR4) (27)], were reduced in satellite cells derived from Dnmt3a-KO mice compared to WT mice. qPCR of individual genes confirmed the microarray results. Expression levels of Myh6, Myh7, and FGFR4 were reduced in satellite cells derived from Dnmt3a-KO mice compared to WT mice (Fig. 6*G*). In addition, we observed increased mRNA expression of Id4 (Fig. 6*G*), a target gene of Gdf5 and inhibitor of muscle cell differentiation (12). The list of genes down-regulated to <0.7-fold in Dnmt3a-KO compared to WT-derived satellite cells is shown in Supplemental Table 4. After performing bioinformatics analysis of the down-regulated genes, we detected a tight junction pathway which may reflect changes in the morphology of the satellite cells from Dnmt3a-KO mice. These data suggest that differentiation was suppressed in satellite cells of Dnmt3a-KO mice compared to WT mice.

TABLE 2. *Pathway analysis*

Pathways	*P*	Benjamini
Hippo signaling pathway	0.013	0.26
p53 signaling pathway	0.075	0.61
TGF-β signaling pathway	0.095	0.55

Compared with WT cells, up-regulated (more than 1.3-fold).

Effect of Gdf5 recombinant protein on gene expression in WT satellite cells

As shown in **Fig. 7*A***, the addition of recombinant Gdf5 protein to the culture medium of WT satellite cells reduced myotube formation. Gdf5 treatment affected neither cell proliferation, assessed by Edu incorporation (Fig. 7*B*), nor the number of myogenin-positive cells (Fig. 7*C*). Nucleus number per myotube (myonuclei, fusion index) decreased with Gdf5 treatment (Fig. 7*D, E*). Length and area of MyHC-positive myotubes decreased in Gdf5-treated cells (Fig. 7*D, E*), suggesting suppressed differentiation. Furthermore, the mRNA expression level of Id4 was increased and Myh6 was reduced (Fig. 7*F*). This is consistent with increased Id4 and decreased Myh6 mRNA expression in satellite cells of Dnmt3a-KO mice with increased Gdf5 mRNA expression. These data suggest that Gdf5 suppresses satellite cell differentiation by increasing Id expression. Together, phenotypes of Dnmt3a-KO cells (Fig. 5) and Gdf5-treated WT cells (Fig. 7) were similar. Thus, Dnmt3a-KO may cause the effects that are at least in part mediated by Gdf5.

DISCUSSION

During atrophy, such as sarcopenia and unloading, muscle regeneration capacity after injury is decreased (9–11). We observed decreased muscle regeneration by denervation (Supplemental Fig. 3). This decreased muscle regeneration capacity is believed to interfere with muscle mass recovery after injury and lead to impaired muscle function as well as more severe sarcopenia with lower quality of life (28). We present a plausible model for the decreased regeneration capacity of atrophied skeletal muscles involving down-regulation of the DNA methyltransferase Dnmt3a in satellite cells and ensuing up-regulation of Gdf5/Bmp14, as well as suppression of satellite cell differentiation. It is better to analyze DNA methylation levels and/or Dnmt3a expression in satellite cells from aged or other atrophy models. However, it is technically difficult because isolation of skeletal muscles and culturing satellite cells in a dish may change their features; for example, loss of connection with extracellular signals causes atrophy. These issues remain to be solved.

Differences in *Gdf5* promoter methylation level between satellite cells and skeletal muscles of Dnmt3a-KO mice

Under normal conditions, we did not observe gross morphologic differences in skeletal muscles between Dnmt3a-KO and WT mice. The DNA methylation level of the *Gdf5* promoter was lower in satellite cells of Dnmt3a-KO mice than in WT mice, while in whole skeletal muscles, *Gdf5* promoter methylation did not differ between Dnmt3a-KO and WT mice (data not shown). Indeed, in skeletal muscles, expression of Gdf5 was very low in both WT and Dnmt3a-KO mice; Gdf5 expression was not significantly increased in skeletal muscles of Dnmt3a-KO mice, which is consistent with the unchanged DNA methylation level (data not shown).

A global search of methylation differences was analyzed using a methylation-sensitive enzyme (*Hpa*II, recognizing the CCGG sequence) (22). We observed 23

TABLE 3. *Genes down-regulated to <0.5-fold in Dnmt3a-KO compared to WT-derived satellite cells by microarray analysis*

Gene	Description	KO/WT, d			
		2	4	5	6
LOC674761	Similar to β myosin heavy chain (LOC674761)	0.2	0.3	0.5	0.2
Myh7	Myosin, heavy polypeptide 7, cardiac muscle, β (Myh7)	0.3	0.3	0.4	0.1
Myh6	Myosin, heavy polypeptide 6, cardiac muscle, α (Myh6)	0.3	0.4	0.4	0.4
Capn6	Calpain 6 (Capn6)	0.3	0.4	0.4	0.5
Dnmt3a	DNA methyltransferase 3A (Dnmt3a)	0.4	0.2	0.2	0.2
Gm608	Predicted gene 608 (Gm608)	0.4	0.4	0.4	0.2
B3galt5	UDP-Gal:betaGlcNAc β 1,3-galactosyltransferase, polypeptide 5 (B3galt5)	0.4	0.3	0.5	0.2
Fgfr4	Fibroblast growth factor receptor 4 (Fgfr4)	0.5	0.3	0.4	0.4
Emid2	EMI domain containing 2 (Emid2)	0.5	0.4	0.4	0.5
ENSMUST00000111103	Collagen α-1 (XXVI) chain Precursor (EMI domain-containing protein 2) (Emilin and multimerin domain-containing protein 2) (Emu2)	0.5	0.4	0.5	0.4
Gtpbp8	GTP-binding protein 8 (putative) (Gtpbp8)	0.5	0.5	0.5	0.4

List of down-regulated genes (<0.5-fold compared to WT mice) in all samples. Numbers show fold changes in gene expression. Expression of Dnmt3a was reduced in Dnmt3a-KO compared to WT cells in all samples. Moreover, expression of Gdf5 was increased in Dnmt3a-KO compared to WT cells in all samples.

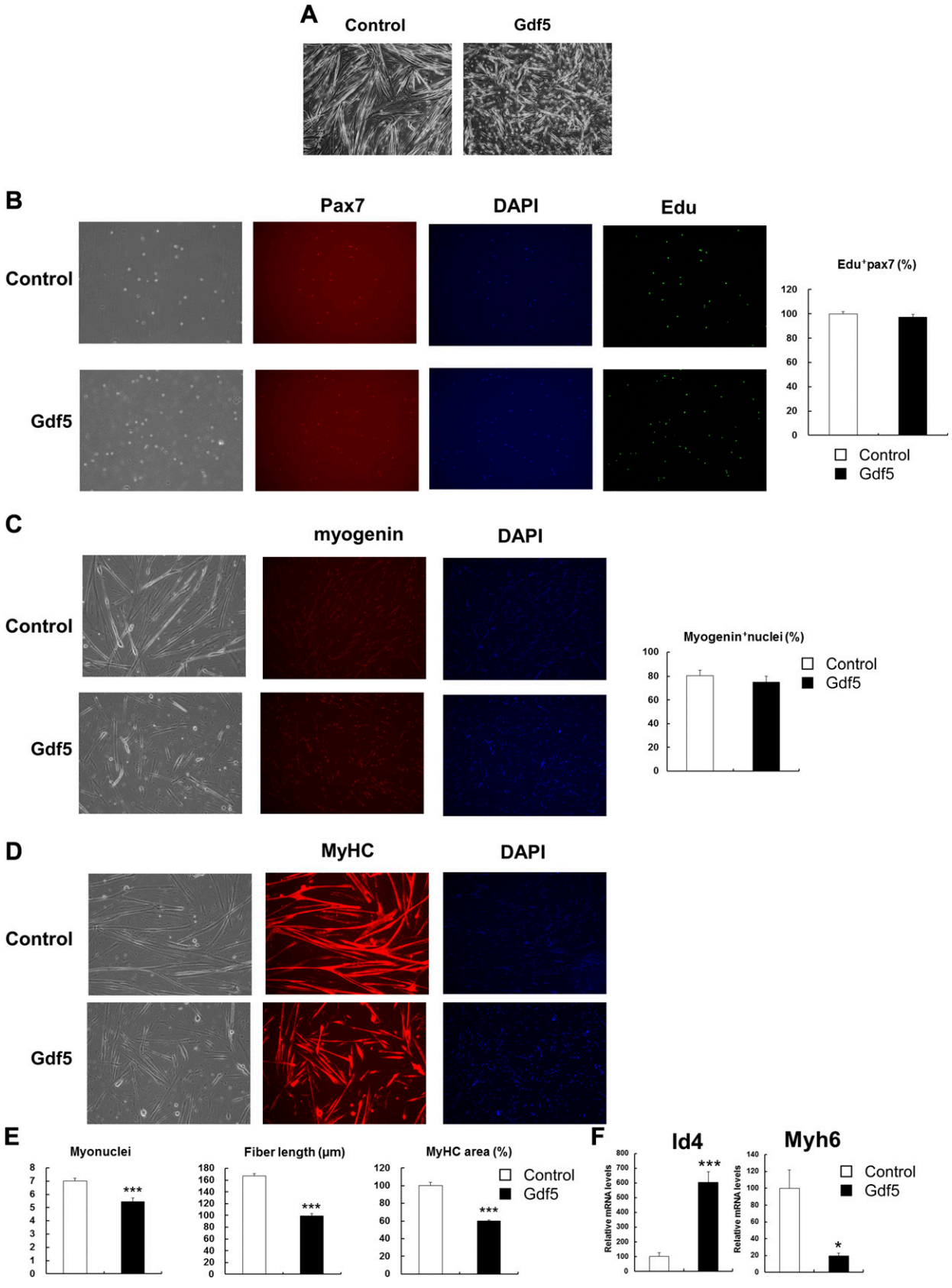

Figure 7. Effect of recombinant Gdf5 in satellite cells from WT mice. *A*) Satellite cells isolated from WT mice were cultured in differentiation medium containing 100 ng/ml Gdf5 recombinant protein for 2 d; photos are representative of bright field images. *B*) Satellite cells were cultured in growth medium for 2 d, then cultured in same medium containing 10 ng/ml Gdf5 recombinant protein for 24 h. Immunostaining of Pax7 (red) in Gdf5-treated WT satellite cells and Edu (green) incorporation during proliferation of cells are shown. Nuclei were stained with DAPI (blue). Ratio of Edu incorporation per Pax7-positive cells

(*continued on next page*)

probes (genes) for skeletal muscles (data not shown) and 155 probes (genes) for satellite cells (Supplemental Table 2) that were markedly less methylated in Dnmt3a-KO mice than in WT mice. Thus, Dnmt3a deletion in skeletal muscles as well as satellite cells is functional. Among the 155 genes in satellite cells, most were not markedly less methylated in skeletal muscles (Supplemental Table 2). Namely, Dnmt3a target genes appear different between skeletal muscles and satellite cells.

Expression of receptors for Gdf5

The known receptors of Gdf5 are Acvr2a, Acvr2b, Bmpr1b, and Bmpr2 (29). Bmpr1b has a high affinity for Gdf5 (29). According to the BioGPS database, containing information on tissue/cell expression patterns of specific mRNAs (*http://biogps.org/*), Acvr2a, Acvr2b, Bmpr1b, and Bmpr2 are expressed in skeletal muscles. Indeed, we observed expression of these receptors in satellite cells as well as in skeletal muscles (Supplemental Fig. 4). Moreover, expression levels of all Gdf5 receptors did not differ between Dnmt3a-KO and WT mice. Thus, Gdf5 is likely to act as an autocrine signal for satellite cells *via* these receptors to suppress differentiation.

Regulation of endogenous Dnmt3a expression

In the present study, we observed a marked reduction in Dnmt3a expression in skeletal muscles in the atrophy model used. One question that remains unanswered is the molecular mechanism underlying the down-regulation of Dnmt3a expression in the atrophy mouse model. It has been reported that Dnmt3a is reduced in the brain (hippocampus and cortex) of aged mice (30). Moreover, Dnmt3a expression is activated by neuronal activity, and partially through the nuclear calcium signaling-dependent pathway (30). In the case of skeletal muscles, calcium ions enter the muscle cells during muscle contraction, which is caused by motor neuron stimulation (31). Stimulation of motor neurons may be important for maintaining Dnmt3a expression in skeletal muscles. Indeed, in our preliminary experiment, treatment with a calcium ionophore significantly increased the expression of Dnmt3a mRNA in C2C12 myoblast cells (data not shown); thus, during muscle atrophy, such as denervation and aging (there is a decline in the number of neuromuscular junctions) (32), Dnmt3a expression may decrease as a result of decreased calcium signaling. Elucidation of the regulation of Dnmt3a expression is an interesting area of research and a focus of our future studies.

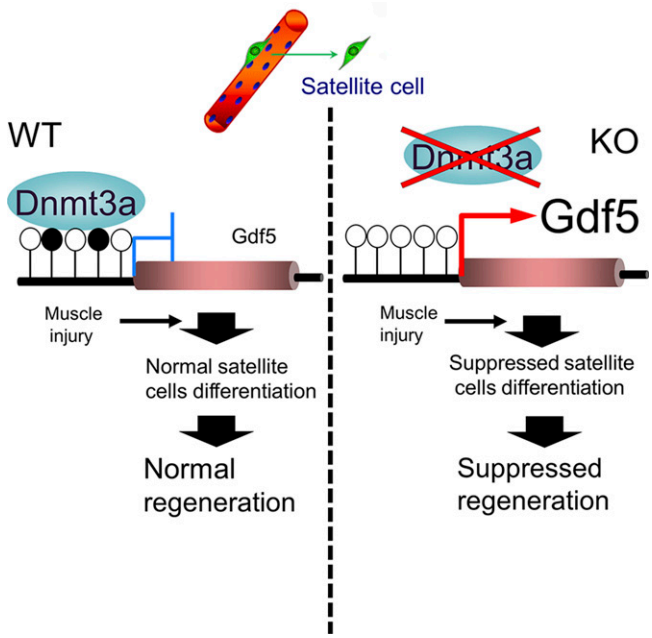

Figure 8. Schematic diagram of summary. In satellite cells, decreased Dnmt3a lead to decreased DNA methylation of *Gdf5* promoter and increased *Gdf5* expression. This released Gdf5 suppresses differentiation of satellite cells. As a result, muscle regeneration, caused by injury, is suppressed in Dnmt3a-KO mice.

Comparison with other studies concerning role of Dnmt3a in skeletal muscles

A few previous studies have examined the role of Dnmt3a in skeletal muscles and satellite cells. Tajrishi *et al.* (8) reported that overexpression of Dnmt3a in skeletal muscles suppressed FGF-inducible 14 (*Fn14*) gene expression and increased the DNA methylation level at the *Fn14* promoter. They also reported that denervation of WT mice decreased Dnmt3a expression and increased Fn14 mRNA expression (8). In our Dnmt3a-KO mice, we did not observe increased Fn14 mRNA expression either in skeletal muscles or satellite cells (data not shown). Thus, knockout of Dnmt3a in this study and overexpression of Dnmt3a in skeletal muscles show different effects on the *Fn14* gene (8). Satellite cell-specific knockout of Dnmt3a using the *Pax7* promoter to drive a Cre-estrogen receptor fusion protein resulted in decreased DNA methylation at the *p57/Kip2* (*Cdkn1c*) gene, a negative regulator of cell proliferation, and increased its expression (33). These results, showing a reduced skeletal muscle regeneration capacity

are shown. *C*, *D*) Satellite cells isolated from WT mice were cultured in differentiation medium containing 10 ng/ml Gdf5 recombinant protein for 2 d. *C*) Immunostaining of myogenin (red) in myotubes from Gdf5-treated WT satellite cells. Ratio of myogenin-positive cells is shown. *D*) Immunostaining of MyHC (red) in myotubes from Gdf5-treated WT satellite cells. *E*) Nucleus number of myotube (myonuclei), myotube length, and ratio of MyHC-positive area per microscopic field. More than 100 myotubes per well were counted in random fields; $n = 3$ (3 individual wells). *F*) mRNA expression was analyzed by qPCR. Cell samples were as used in *A*; $n = 3$ per group. Data represent means ± SEM. $^{*}P < 0.05$, $^{***}P < 0.001$ (unpaired, 2-tailed Student's *t* test).

(33), are consistent with our study. While we observed decreased methylation levels of the *p57/Kip2* promoter region in the global search of methylation differences (Supplemental Table 2), we did not observe increased p57/Kip2 mRNA expression in the satellite cells of our Dnmt3a-KO mice (data not shown). There was no difference in the satellite cell proliferation rate between WT and Dnmt3a-KO mice as accessed by an EdU assay (Fig. 5*B*). This difference could result from the subtle culture conditions or the use of different promoters for Cre expression, as this would affect the timing and location of expression.

CONCLUSIONS

We summarize our results and conclusions in **Fig. 8**. On the basis of the Dnmt3a-KO data, in satellite cells, decreased Dnmt3a leads to decreased DNA methylation of the *Gdf5* promoter. Loss of Dnmt3a causes desuppression of the *Gdf5* promoter, resulting in increased Gdf5 expression and enhanced secretion. This released Gdf5 binds to its receptors on satellite cells and suppresses their differentiation. Decreased Dnmt3a and increased Gdf5 can explain, at least in part, the delayed or impaired regeneration and recovery of skeletal muscle mass after injury during atrophy including aging. FJ

ACKNOWLEDGMENTS

Microarray data analysis was in part performed at the Medical Research Support Center, Graduate School of Medicine, Kyoto University. This study was supported by Grants-in-Aid for Scientific Research (KAKENHI) from the Japanese Ministry of Education, Culture, Sports, Science, and Technology (MEXT), and by the Council for Science, Technology, and Innovation (CSTI), Cross-Ministerial Strategic Innovation Promotion Program (SIP), and Technologies for Creating Next-Generation Agriculture, Forestry, and Fisheries (funding agency: Bio-oriented Technology Research Advancement Institution; NARO). This study was also supported in part by the program of the Joint Usage/Research Center for Developmental Medicine, Institute of Molecular Embryology and Genetics, Kumamoto University. The funders had no role in the study design, data collection and analysis, decision to publish, and preparation of the article. The authors declare no conflicts of interest.

AUTHOR CONTRIBUTIONS

Y. Hatazawa, Y. Ono, M. Okano, Y. Kamei, and Y. Ogawa conceived and designed the experiments; Y. Hatazawa, Y. Ono, Y. Hirose, S. Kanai, N. L. Fujii, S. Machida, I. Nishino, T. Shimizu, and Y. Kamei performed the experiments; Y. Hatazawa, Y. Ono, Y. Hirose, N. L. Fujii, S. Machida, I. Nishino, T. Shimizu, and Y. Kamei analyzed the data; Y. Hatazawa, Y. Ono, Y. Hirose, N. L. Fujii, S. Machida, I. Nishino, T. Shimizu, M. Okano, Y. Kamei, and Y. Ogawa contributed reagents and materials/analysis tools; and Y. Hatazawa, Y. Kamei, and Y. Ogawa wrote the article.

REFERENCES

1. Guasconi, V., and Puri, P. L. (2008) Epigenetic drugs in the treatment of skeletal muscle atrophy. *Curr. Opin. Clin. Nutr. Metab. Care* **11**, 233–241
2. Maunakea, A. K., Nagarajan, R. P., Bilenky, M., Ballinger, T. J., D'Souza, C., Fouse, S. D., Johnson, B. E., Hong, C., Nielsen, C., Zhao, Y., Turecki, G., Delaney, A., Varhol, R., Thiessen, N., Shchors, K., Heine, V. M., Rowitch, D. H., Xing, X., Fiore, C., Schillebeeckx, M., Jones, S. J., Haussler, D., Marra, M. A., Hirst, M., Wang, T., and Costello, J. F. (2010) Conserved role of intragenic DNA methylation in regulating alternative promoters. *Nature* **466**, 253–257
3. Wu, H., Coskun, V., Tao, J., Xie, W., Ge, W., Yoshikawa, K., Li, E., Zhang, Y., and Sun, Y. E. (2010) Dnmt3a-dependent nonpromoter DNA methylation facilitates transcription of neurogenic genes. *Science* **329**, 444–448
4. Okano, M., Bell, D. W., Haber, D. A., and Li, E. (1999) DNA methyltransferases Dnmt3a and Dnmt3b are essential for *de novo* methylation and mammalian development. *Cell* **99**, 247–257
5. Taylor, S. M., and Jones, P. A. (1979) Multiple new phenotypes induced in 10T1/2 and 3T3 cells treated with 5-azacytidine. *Cell* **17**, 771–779
6. Liu, R., Kim, K. Y., Jung, Y. W., and Park, I. H. (2016) Dnmt1 regulates the myogenic lineage specification of muscle stem cells. *Sci. Rep.* **6**, 35355
7. Xie, S., Wang, Z., Okano, M., Nogami, M., Li, Y., He, W. W., Okumura, K., and Li, E. (1999) Cloning, expression and chromosome locations of the human DNMT3 gene family. *Gene* **236**, 87–95
8. Tajrishi, M. M., Shin, J., Hetman, M., and Kumar, A. (2014) DNA methyltransferase 3a and mitogen-activated protein kinase signaling regulate the expression of fibroblast growth factor–inducible 14 (Fn14) during denervation-induced skeletal muscle atrophy. *J. Biol. Chem.* **289**, 19985–19999
9. Ehrhardt, J., and Morgan, J. (2005) Regenerative capacity of skeletal muscle. *Curr. Opin. Neurol.* **18**, 548–553
10. D'Souza, D. M., Zhou, S., Rebalka, I. A., MacDonald, B., Moradi, J., Krause, M. P., Al-Sajee, D., Punthakee, Z., Tarnopolsky, M. A., and Hawke, T. J. (2016) Decreased satellite cell number and function in humans and mice with type 1 diabetes is the result of altered Notch signaling. *Diabetes* **65**, 3053–3061
11. Mozdziak, P. E., Truong, Q., Macius, A., and Schultz, E. (1998) Hindlimb suspension reduces muscle regeneration. *Eur. J. Appl. Physiol. Occup. Physiol.* **78**, 136–140
12. Ono, Y., Calhabeu, F., Morgan, J. E., Katagiri, T., Amthor, H., and Zammit, P. S. (2011) BMP signalling permits population expansion by preventing premature myogenic differentiation in muscle satellite cells. *Cell Death Differ.* **18**, 222–234
13. Rider, C. C., and Mulloy, B. (2010) Bone morphogenetic protein and growth differentiation factor cytokine families and their protein antagonists. *Biochem. J.* **429**, 1–12
14. Reynard, L. N., Bui, C., Canty-Laird, E. G., Young, D. A., and Loughlin, J. (2011) Expression of the osteoarthritis-associated gene *GDF5* is modulated epigenetically by DNA methylation. *Hum. Mol. Genet.* **20**, 3450–3460
15. Kamei, Y., Miura, S., Suzuki, M., Kai, Y., Mizukami, J., Taniguchi, T., Mochida, K., Hata, T., Matsuda, J., Aburatani, H., Nishino, I., and Ezaki, O. (2004) Skeletal muscle FOXO1 (FKHR) transgenic mice have less skeletal muscle mass, down-regulated type I (slow twitch/red muscle) fiber genes, and impaired glycemic control. *J. Biol. Chem.* **279**, 41114–41123
16. Kaneda, M., Okano, M., Hata, K., Sado, T., Tsujimoto, N., Li, E., and Sasaki, H. (2004) Essential role for *de novo* DNA methyltransferase Dnmt3a in paternal and maternal imprinting. *Nature* **429**, 900–903
17. Brennan, K. J., and Hardeman, E. C. (1993) Quantitative analysis of the human alpha-skeletal actin gene in transgenic mice. *J. Biol. Chem.* **268**, 719–725
18. Miura, S., Tomitsuka, E., Kamei, Y., Yamazaki, T., Kai, Y., Tamura, M., Kita, K., Nishino, I., and Ezaki, O. (2006) Overexpression of peroxisome proliferator-activated receptor gamma co-activator-1alpha leads to muscle atrophy with depletion of ATP. *Am. J. Pathol.* **169**, 1129–1139
19. Ono, Y., Urata, Y., Goto, S., Nakagawa, S., Humbert, P. O., Li, T. S., and Zammit, P. S. (2015) Muscle stem cell fate is controlled by the cell-polarity protein Scrib. *Cell Reports* **10**, 1135–1148
20. Srinivas, S., Watanabe, T., Lin, C. S., William, C. M., Tanabe, Y., Jessell, T. M., and Costantini, F. (2001) Cre reporter strains produced by targeted insertion of EYFP and ECFP into the ROSA26 locus. *BMC Dev. Biol.* **1**, 4

21. Hatazawa, Y., Tadaishi, M., Nagaike, Y., Morita, A., Ogawa, Y., Ezaki, O., Takai-Igarashi, T., Kitaura, Y., Shimomura, Y., Kamei, Y., and Miura, S. (2014) PGC-1α-mediated branched-chain amino acid metabolism in the skeletal muscle. *PLoS One* **9**, e91006
22. Ehara, T., Kamei, Y., Yuan, X., Takahashi, M., Kanai, S., Tamura, E., Tsujimoto, K., Tamiya, T., Nakagawa, Y., Shimano, H., Takai-Igarashi, T., Hatada, I., Suganami, T., Hashimoto, K., and Ogawa, Y. (2015) Ligand-activated PPARα-dependent DNA demethylation regulates the fatty acid β-oxidation genes in the postnatal liver. *Diabetes* **64**, 775–784
23. Kumaki, Y., Oda, M., and Okano, M. (2008) QUMA: quantification tool for methylation analysis. *Nucleic Acids Res.* **36**(Web Server), W170–W175
24. Egerman, M. A., Cadena, S. M., Gilbert, J. A., Meyer, A., Nelson, H. N., Swalley, S. E., Mallozzi, C., Jacobi, C., Jennings, L. L., Clay, I., Laurent, G., Ma, S., Brachat, S., Lach-Trifilieff, E., Shavlakadze, T., Trendelenburg, A. U., Brack, A. S., and Glass, D. J. (2015) GDF11 increases with age and inhibits skeletal muscle regeneration. *Cell Metab.* **22**, 164–174
25. Zammit, P. S., Relaix, F., Nagata, Y., Ruiz, A. P., Collins, C. A., Partridge, T. A., and Beauchamp, J. R. (2006) Pax7 and myogenic progression in skeletal muscle satellite cells. *J. Cell Sci.* **119**, 1824–1832
26. Suchak, A., Hunt, N. P., Shah, R., Sinanan, A. C., Lloyd, T., and Lewis, M. P. (2009) Myosin proteins identified from masseter muscle using quantitative reverse transcriptase–polymerase chain reaction—a pilot study of the relevance to orthodontics. *Eur. J. Orthod.* **31**, 196–201
27. Zhao, P., Caretti, G., Mitchell, S., McKeehan, W. L., Boskey, A. L., Pachman, L. M., Sartorelli, V., and Hoffman, E. P. (2006) Fgfr4 is required for effective muscle regeneration *in vivo*. Delineation of a MyoD-Tead2-Fgfr4 transcriptional pathway. *J. Biol. Chem.* **281**, 429–438
28. Grounds, M. D. (1998) Age-associated changes in the response of skeletal muscle cells to exercise and regeneration. *Ann. N. Y. Acad. Sci.* **854**, 78–91
29. Nishitoh, H., Ichijo, H., Kimura, M., Matsumoto, T., Makishima, F., Yamaguchi, A., Yamashita, H., Enomoto, S., and Miyazono, K. (1996) Identification of type I and type II serine/threonine kinase receptors for growth/differentiation factor-5. *J. Biol. Chem.* **271**, 21345–21352
30. Oliveira, A. M., Hemstedt, T. J., and Bading, H. (2012) Rescue of aging-associated decline in Dnmt3a2 expression restores cognitive abilities. *Nat. Neurosci.* **15**, 1111–1113
31. Salanova, M., Volpe, P., and Blottner, D. (2013) Homer protein family regulation in skeletal muscle and neuromuscular adaptation. *IUBMB Life* **65**, 769–776
32. Rudolf, R., Khan, M. M., Labeit, S., and Deschenes, M. R. (2014) Degeneration of neuromuscular junction in age and dystrophy. *Front. Aging Neurosci.* **6**, 99
33. Naito, M., Mori, M., Inagawa, M., Miyata, K., Hashimoto, N., Tanaka, S., and Asahara, H. (2016) Dnmt3a regulates proliferation of muscle satellite cells *via* p57Kip2. *PLoS Genet.* **12**, e1006167

Received for publication June 21, 2017.
Accepted for publication October 30, 2017.

Reduced Dnmt3a increases Gdf5 expression with suppressed satellite cell differentiation and impaired skeletal muscle regeneration

Yukino Hatazawa, Yusuke Ono, Yuma Hirose, et al.

FASEB J published online November 16, 2017
Access the most recent version at doi:10.1096/fj.201700573R